


100- to about 1000-Angstroms, and most preferably
about 400-Angstroms.

REMARKS

The specification for the above-referenced patent application was reviewed, and a number of inadvertent spelling, grammatical and formal issues were noted. These issues are addressed by the foregoing amendments. It is respectfully requested that these amendments be entered prior to examination on the merits.


CERTIFICATE OF MAILING

I hereby certify that this correspondence is being deposited with the U.S. Postal Service as first class mail in an envelope addressed to: BOX NON-FEE AMENDMENT, Commissioner for Patents, Washington, D.C. 20231, on June 1, 2001.


Paul W. Churilla
Date of Signature: June 1, 2001

Respectfully submitted,

KOLISCH, HARTWELL, DICKINSON,
McCORMACK & HEUSER


Paul W. Churilla
Registration No. 47,495
of Attorneys for Applicant
520 S.W. Yamhill Street, Suite 200
Portland, Oregon 97204
Telephone: (503) 224-6655
Facsimile: (503) 295-6679

VERSION WITH MARKINGS TO SHOW CHANGES MADE

In the Specification:

Marked-up paragraph beginning on page 2, line 5 and ending on page 2, line 15:

Generally, sputtering can be characterized as a well-controlled, well-engineered process. Sputtering cathodes, power supplies, and source material targets are available from several vendors. Sputtering has been successfully applied in several thin-film applications including deposition of impermeable films on food packaging, low emissivity (low-e) coatings on residential and commercial plate glass, and decorative coatings. Control of sputtered film uniformity has been engineered into the cathode structure. Negative aspects of sputtering including the high cost of the sputtering systems, that the source (target) utilization is generally poor (20 to 40%), and that there are temporal limitations in creating multi-component films (i.e., more than three elements). More specifically, to sputter multi-component films, individual layers are usually deposited followed by a heat treatment cycle to react the components together, which may require considerable time.

Marked-up paragraph beginning on page 3, line 5 and ending on page 3, line 8:

As noted above, complex multi-element films are difficult to produce using currently available techniques of sputtering or evaporation. [This]The invention described herein provides a new class of evaporation principles and associated

evaporation sources resulting in the creation of uniform, well controlled multi-element thin films.

Marked-up paragraph beginning on page 4, line 8 and ending on page 4, line 21:

Although commercial use and interest in thin-film photovoltaics has increased dramatically over the past five years, commercial wide-scale use of thin film PVs for bulk power generation historically has been limited due to PV's low performance and high cost. In recent years, however, performance has been less of a limiting factor as dramatic improvements in PV module efficiency have been achieved with both crystalline silicon and thin-film photovoltaics. The laboratory scale efficiency of crystalline silicon is approaching 20%. Modules ranging from 10 to 14% are currently commercially available from several vendors. Similarly, laboratory scale efficiencies of above 10% have been achieved with thin-film PV devices of copper indium diselenide, cadmium telluride, and amorphous silicon. The efficiency of a thin film copper-indium-gallium-diselenide (CIGS) PV device is now approaching 19%. Additionally, several companies have achieved thin-film large area module efficiencies ranging from 8 to 12%. These recent improvements in efficiency have greatly reduced performance concerns leaving cost as the primary deterrent preventing wide-scale commercial application of PV modules for electricity generation.

Marked-up paragraph beginning on page 5, line 1 and ending on page 5, line 7:

Thin-film photovoltaics, namely amorphous silicon, cadmium telluride, and copper[]-indium[]-diselenide (CIS), offer reduced cost by employing deposition techniques widely used in the thin-film industry for protective, decorative, and functional coatings. Common examples of low cost commercial thin-film products include water permeable coatings on polymer-based food packaging, decorative coatings on architectural glass, low emissivity thermal control coatings on residential and commercial glass, and scratch and anti-reflective coatings on eyewear.

Marked-up paragraph beginning on page 5, line 8 and ending on page 5, line 13:

Of all thin film PV compositions, CIGS has demonstrated the greatest potential for high performance and low cost. More specifically, CIGS has achieved the highest laboratory efficiency (18.8% by NREL), is stable, has low toxicity, and is truly thin-film (requiring less than two microns layer thickness). These characteristics allow for the large-scale low cost manufacturing of CIGS PV_s thereby enabling the penetration by thin-film PV_s into bulk power generation markets.

Marked-up paragraph beginning on page 5, line 15 and ending on page 6, line 7:

The overall efforts that surround the developments that are specifically addressed in this document have introduced a significant collection of innovations that apply to improved low-cost, large-scale manufacturing to the field of photovoltaics and

thin films. Generally speaking, several key areas of these innovations include: (1) a general fabrication procedure, including a preferably roll-to-roll-type, process-chamber-segregated, “continuous-motion”, method for producing such a structure; (2)[,] a special multi-material vapor-deposition environment which is created to implement an important co-evaporation, layer-deposition procedure performed in and part of the method just mentioned; (3)[,] a structural system uniquely focused on creating a vapor environment generally like that just referred to; (4)[,] an organization of method steps involved in the generation of such a vapor environment; (5)[,] a unique, vapor-creating, materials-distributing system, which includes specially designed heated crucibles with carefully arranged, spatially distributed, localized and generally point-like, heated-nozzle sources of different metallic vapors, and a special multi-fingered, comb-like, vapor-delivering manifold structure.

Marked-up paragraph beginning on page 6, line 9 and ending on page 6, line 10:

Fig. 1 is a simplified schematic elevation generally illustrating process steps and stages employed for creating a photovoltaic (PV) module.

Marked-up paragraph beginning on page 7, line 1 and ending on page 7, line 4:

Fig. 6, is a simplified, schematic side elevation illustrating a chamber wherein one format of copper-indium-gallium-diselenide (CIGS) or copper-indium-diselenide (CIS) roll-to-roll strip processing occurs according to the disclosed

embodiment, with this one format involving movement of strip material past three vapor-plume-creating stations.

Marked-up paragraph beginning on page 7, line 10 and ending on page 7, line 12:

Fig. 10 is a fragmentary schematic perspective view of a vapor-deposition zone R wherein certain vapor-creating and vapor-presence phenomena exist and take place within the chamber [pictured]illustrated in Figs. 6, 7 and 8.

Marked-up paragraph beginning on page 7, line 13 and ending on page 7, line 18:

Fig. 11 illustrates two or three roll-to-roll chamber-processing steps. Specifically, Fig. 11 can be viewed as illustrating (a) a step of applying a layer of cadmium-sulfide (CdS), (b) a step, when employed, of applying a layer of intrinsic-zinc-oxide (i-ZnO), and (c) a step of applying a conductive-oxide layer, such as a zinc-oxide:aluminum (ZnO:Al) layer. This single-view, “multiple-purpose” drawing figure is employed in the interest of simplifying the overall collection of drawings.

Marked-up paragraph beginning on page 9, line 18 and ending on page 9, line 18:

Fig. 31 pictorially illustrates flow of [the]a vapor through an orifice.

Marked-up paragraph beginning on page 10, line 14 and ending on page 10, line 18:

Fig. 1 illustrates the steps involved preferably in making a new kind of photovoltaic (PV) module in a roll-to-roll, continuous-motion process in accordance with

the present invention. Those skilled in the art should understand that, while roll-to-roll, continuous motion processing is employed in the described embodiment, non-roll-to-roll procedures could be used effectively in certain applications.

Marked-up paragraph beginning on page 11, line 17 and ending on page 12, line 2:

Nine separate individual processing chambers 22, 24, 26 23, 25, 27, 28, 30, 29 are illustrated as rectangular blocks in Fig. 1. The various layers of materials that are used to form a PV module according to this invention are applied or modified in these chambers. The relative sizes of these blocks as pictured in Fig. 1 are not important. It should be noted that the steps represented by some of the processing chambers are optional in some applications. For instance, the intrinsic-zinc-oxide (i-ZnO) layer created in chamber 28 may be omitted.

Marked-up paragraph beginning on page 12, line 3 and ending on page 12, line 10:

Processing begins with a bare starter roll, or strip, of elongate thin-film, flexible substrate material, preferably polyimide (PI), which is supplied from pay-out roll 10. This uncoated material might typically have a width of about 33-cm, a thickness of about 0.005-cm, and a length of up to about 300-meters. The width, thickness and length dimensions are, of course, matters of choice, depending on the ultimate intended application for finished PV modules. One PI material suitable for use in the disclosed system, is Upilex S – a material currently available commercially from KISCO in Santa Clara, CA.

Marked-up paragraph beginning on page 13, line 1 and ending on page 13, line 5:

A stress-compliant metal interlayer, preferably nickel-vanadium (Ni-V), chosen to have intermediate thermal expansion characteristics between the PI and a subsequently-applied molybdenum (Mo) layers can be optionally utilized as the first layer deposited onto the PI. This step is not illustrated in Fig. 1, but can either be accomplished in a chamber similar in construction to chamber 22 or within a separate processing zone in chamber 22.

Marked-up paragraph beginning on page 13, line 6 and ending on page 13, line 13:

Within chamber 22, and in a manner that will be more fully discussed shortly, two layers of Mo, each containing entrained oxygen, and each possessing a certain level of intentionally created, desired, internal compressive stress, are formed on the opposite sides, or faces, of PI strip 32. These two layers are shown on the opposite faces (top and bottom in Fig. 1) of fragment 32 at 34, 36 above chamber 22. Layer 34 forms a back contact layer for the PV module of the present invention. In the case of a stainless steel substrate strip, the Mo back contact layer would normally be replaced with a chromium/molybdenum (Cr/Mo) bilayer.

Marked-up paragraph beginning on page 14, line 18 and ending on page 14, line 22:

In chamber 26, a window or buffer layer in the form of cadmium-sulfide (CdS) is applied as a layer 40 extending over the CIGS or CIS layer that was formed in

chamber 24. The CdS layer is preferably applied in a non-wet manner by radio-frequency (RF) sputtering. This results in an overall multiple-layer structure such as pictured generally above chamber 26.

Marked-up paragraph beginning on page 15, line 18 and ending on page 15, line 21:

If the optional, electrically insulating, intrinsic-zinc-oxide (i-ZnO) layer is employed, this is prepared in processing chamber 28 to create a layer arrangement such as that pictured above chamber 28. In this layer arrangement, the i-ZnO layer is shown at 42, overlying the CdS layer.

Marked-up paragraph beginning on page 16, line 6 and ending on page 16, line 11:

Where an insulating i-ZnO layer, such as layer 42, is created, the resulting overall layer structure includes what is referred to later herein as a sandwich substructure, indicated generally by arrows 46 in Fig. 1. Substructure 46 includes the i-ZnO layer sandwiched between the CdS layer and the zinc-oxide:aluminum (ZnO:Al) layer. Thus, where such a sandwich substructure is employed, a contiguous protective intermediary layer (i-ZnO) is provided interposed between the CIGS/CIS layer and the top contact layer 44.

Marked-up paragraph beginning on page 16, line 12 and ending on page 16, line 20:

Fig. 3 illustrates a PV-cell structure 47, such as produced from the process outlined in Fig. 1. It should be noted that the layer thicknesses are not drawn to scale. The

specific layer arrangement which makes up device 47 includes, a stress neutralizing back side coating, a PI substrate 32, a stress compliant-intermediate coefficient of thermal expansion (CTE) Ni-alloy layer, oxygen-entraining and internally-compressed Mo layers 34, 36, CIGS or CIS layer 38, CdS layer 40, i-ZnO layer 42, and overlying, transparent conductive-oxide, ZnO:Al layer 44. This is a device wherein the option to employ i-ZnO has been elected. The sandwich substructure 46 mentioned earlier, which includes this i-ZnO layer, is identified with a bracket which bears reference numeral 46 in Fig. 3.

Marked-up paragraph beginning on page 18, line 1 and ending on page 18, line 11:

Monolithic integration creates a large building block, referred to as a submodule used to create a final module with desired voltage and current for the expected application. Building block size may be 30x30-cm, but is, of course, a matter of choice depending on the starting strip material size and the anticipated end-use of the product[ion]. At appropriate points in time during the overall processing procedure which has just been generally outlined in the ‘monolithic interconnection’ discussion, the functional electrical circuitry which is required in the end-product PV module structure is prepared. This circuitry establishes the needed electrical interconnects between adjacent submodules. The specific monolithic interconnection patterning configuration employed, and the technique(s) for creating such a configuration, are matters of choice, and are well known to those versed in the art.

Marked-up paragraph beginning on page 21, line 8 and ending on page 21, line 18:

After heat treating processing begins by transporting the dried polyimide material through chamber 22. Ni-V alloy has proven to be suitable for the metal interlayer. However any stress compliant metal, with a [CTE] coefficient of thermal expansion (CTE) intermediate to that of the flexible substrate and the back electrical contact could be employed. Preferred materials are [N] nickel based alloys that have enough alloying element to render the Ni non-magnetic but retain the Ni stress compliance, intermediate CTE, low bulk resistivity, and doesn't react with the overlying Mo. Examples include nickel alloyed with 0 to 10 weight percent vanadium, nickel alloyed with 0 to 15 weight percent molybdenum, and Ni alloyed with 0 to 7 [wt] weight percent chromium. Additionally, alternative metals that have the characteristic of intermediate CTE and low resistivity could be used. Examples include copper and copper alloys including brass, niobium, chromium, tantalum, and titanium.

Marked-up paragraph beginning on page 21, line 19 and ending on page 22, line 2:

In each of stations 64, 66, the Ni alloy source employed for the stress compliant layer sputter-deposition preferably takes the form of a 99.95% sintered Ni with [a] 7 weight percent vanadium block, for example, which is commercially available from Pure Tech Inc., Carmel, NY. For this Ni-7V source material the sputtering cathodes are suitably (and conventionally) operated at power levels ranging from 1 to 10kW each, with 4.0-kW each being most preferable.

Marked-up paragraph beginning on page 22, line 3 and ending on page 22, line 10:

Processing further proceeds with the formation/deposition of the two previously discussed Mo layers on opposing faces of the PI web. The Mo layers are formed by a Mo-deposition plasma generated inside the chamber 22 (Fig. 5). In each of stations 64, 66, the Mo source employed for Mo sputter-deposition preferably takes the form of a 99.95% pure vacuum arc cast Mo block, for example, one which is commercially available from Climax Specialty Metals of Cleveland, Ohio. For this Mo source material the sputtering cathodes are suitably (and conventionally) operated at power levels ranging from 1 to 10kW each, with [a] 4.0-kW each being most preferable.

Marked-up paragraph beginning on page 22, line 11 and ending on page 23, line 3:

In each of sputtering stations 64, 66, the spacing between the strip material and the Mo source material is arranged to be about 1- to about 20-cm, and most preferably about 10-cm. These spacing considerations play an important role in ensuring that the local deposition regions defined between the substrate and the Mo source material are especially suited to promote the introduction of appropriate compressive stress into the forming Mo layers. Within these regions, the pressure of argon gas increases and decreases, respectively, as the distance between the substrate and the sources decreases and increases. The preferable spacing distances and the chamber pressures stated above assure a condition in chamber 22 which causes the activity of argon atoms to promote a slight, but desirable, level of internal compressive stress in each

of the two, forming Mo layers. It is believed that this compressive stress comes into being [is that argon] as a result of the fact that argon atoms “hammer” and effectively “ball-peen” the forming Mo layers. As described in more detail below, the internal compressive stress tends to counteract the tension imparted in the Mo layers that would otherwise occur as the strip is heated and the PI expands during the CIGS processing described later.[.]

Marked-up paragraph beginning on page 23, line 9 and ending on page 23, line 21:

We have found, as at least one component of the present invention, that a solution to this problem involves the addition of the mentioned entrained oxygen to the Mo layers. It is believed that the oxygen introduced into chamber 22 according to the present invention occupies the interstitial site of the BCC unit cell. Oxygen present at interstitial sites creates a higher level of internal [intrinsic] compressive stress. Because the coefficient of thermal expansion of the PI is much greater than that of the Mo, the high level of compressive stress is necessary to ensure the Mo remains in compression during heating in the CIGS chamber. If the Mo is not [in] subject to enough compression, the thermal expansion mismatch between the PI and Mo would cause the Mo to transition into tension in the CIGS chamber and create cracking within the Mo. The introduced oxygen contributes to the act of creating internal compressive stress in the Mo layers. As a consequence, the Mo layers become more tolerant to bending and more resistant to cracking.

Marked-up paragraph beginning on page 24, line 1 and ending on page 24, line 5:

Thus, two principles are applied here to increase the compressive stress within the Mo: 1.) the combination of low sputtering pressure and short target-to-substrate spacing creates reflected neutral argon peening which imparts an[d] intrinsic high state of compression in the Mo film; and 2.) the addition of oxygen to create a higher level of [intrinsic] internal compressive stress in the Mo.

Marked-up paragraph beginning on page 26, line 13 and ending on page 26, line 22:

When the entire strip of material has finished its processing transport within chamber 22, and has been collected on take-up roll 60, the latter is removed from chamber 22, and placed in chamber 24 (see now Figs. 6-8, 10 and 12-14) to become the operative pay-out roll in that chamber. The strip material feeds in the direction of arrow 16 from pay-out roll 60 to a downstream take-up roll 68 in chamber 24. As the strip material moves through chamber 24, the absorber CIGS or CIS layer 38 is formed on Mo layer 34. [Transport-guide] A transport-guide structure (not shown) is employed between rolls 60, 68 in chamber 24 to support and guide the strip. The short, open arrow which appears at the left side of the block representation of chamber 24 in Fig. 6 symbolizes the hardware provided for the delivery of appropriate constituent substances to chamber 24.

Marked-up paragraph beginning on page 27, line 1 and ending on page 27, line 16:

It is within chamber 24, and specifically within a deposition zone R, that the unique molten-liquid-to-vapor co-evaporation process mentioned above for establishing a CIGS or a CIS layer is performed. Figs. 6-8 and 10 illustrate schematically a configuration for, and certain environmental conditions within, the inside of chamber 24. Chamber 24 is designed specifically for the creation (according to one way of practicing this stage of the present invention) of a CIGS (rather than a CIS) layer. Accordingly, pictured as small blocks and tiny circles (Fig. 6 only) distributed along the bottom of chamber 24, are structures, designated 70, 72, 74, 76, 78, 79, 81, which function to generate vapors of copper (70), gallium (72) indium (74) and selenium (76, 78, 79, 81) for deposition. Structures 70-81 form the bulk of the vapor-deposition-creating system 83 of the present invention. One of the features that distinguishes this embodiment is that the vapor deposition environment created in Zone R is a continuum of evaporant fluxes as opposed a step-wise processes. Within Zone R, fluxes are held constant and by translation over the sources the [reception] receiving elongate substrate encounters a varying flux of material specifically designed to achieve optimum performance in the CIGS layer.

Marked-up paragraph beginning on page 28, line 5 and ending on page 28, line 14:

[Direction] Directing attention now particularly to Figs. 16-19, along with Fig. 9, a description now immediately follows which explains the constructions of

Page 39 – PRELIMINARY AMENDMENT; Serial No. 09/613,951

effusion sources 70, 72, 74 in more detail. Each of these effusion sources is substantially the same in construction. Accordingly, description now proceeds with reference made specifically (where appropriate) only to effusion source 70. At the onset of this description of effusion sources construction, we should note that other specific effusion sources configurations, with more or less than four principal parts, could be used if desired. The effusion source construction parameters set forth and referred to herein, should amply guide those skilled in the art toward the making and using of other, alternative effusion sources structures.

Marked-up paragraph beginning on page 29, line 8 and ending on page 29, line 17:

Each of effusion source shells 100 has a [long] length dimension herein of about 45-cm, a width dimension (measured along the long axis of chamber 24) of about 7-cm, and a height dimension of about 7-cm. Length and width can be either proportionally or non-proportionally scaled to match the zone R and substrate with dimensions, and are matters of choice. From longitudinal centerline-to-centerline of adjacent effusion sources, a preferred distance is about 8.9-cm. Similar to the effusion source size the centerline-to-centerline spacing can be adjusted to the Zone R dimensions and to the substrate width and are matters of choice. However, from a “plan view” perspective of the effusion source nozzle organization, this structure is generally centered with respect to the footprint of zone R.

Marked-up paragraph beginning on page 34, line 17 and ending on page 35, line 6:

Fig. 10, in dashed lines, shows representative plumes 70a, 72a which emanate from effusion sources 70, 72, respectively, as if to form, nominally, what we sometimes refer to as a vapor-tufted environment, such as was generally mentioned earlier. Use of the word “tufted” herein is made simply to evoke visualization of how a co-mingled deposition-vapor fog comes into being in chamber 24. The copper, gallium and indium vapor plumes that exist during CIGS deposition in chamber 24 are [taught] thought to be a vector quantity in the shape of the form $\sin^2 \theta$ as shown in Fig. 32. Effusion from a single orifice source is essentially the sum of two processes. The first of these is the evaporation of the source material, the second is the flow of the vapor through the orifice as pictorially shown in Fig. 31. Each of these processes provides a “resistance” to the effusion of the source material. Evaporation of the source materials will be described later.

Marked-up paragraph beginning on page 39, line 12 and ending on page 40, line 4:

In accordance with a preferred embodiment of the system of the present invention, the molten temperature of copper within crucible 70 is suitably maintained in the range of about 1400°C to about 1700°C, and most preferably at a temperature of about 1565°C (+/- about 1°C). The temperature of the molten gallium within crucible 72 is suitably maintained within the range of about 1000°C to about 1350°C, and most preferably at about 1225°C (+/- about 1°C). Finally, the temperature of the molten indium within crucible 74 is most appropriately (according to what we have learned in our practice of use of this invention) maintained in the range of about 950°C to about 1300°C,

and most preferably at about 1205°C (+/- about 1°C). The temperature of molten selenium in reservoir 85b is preferably maintained in the range of about 275°C to about 500°C, and most preferably to about 415°C (+/- about 10°C). Although these temperatures are in the preferred range for the disclosed sources with 0.95-cm orifices, the rate restricting nozzle principals outlined herein indicated that as the orifice size increases, the temperature would decrease to achieve a constant rate, or alternatively, as the orifice decreases, the temperature would increase to achieve a constant rate.

Marked-up paragraph beginning on page 44, line 6 and ending on page 44, line 16:

Separate chambers are also beneficial because of the substantial differences in environment between separate zones, i.e., Mo is typically done [done with] at ~1.5 mtorr with argon and water, CIGS is typically done at 0.001 mtorr with no argon or water, CdS is typically done at 2 mtorr with just argon. With a combined chamber, a lock is used to stabilize the environment before the valves separating the zones from the lock is opened. For example, as the lock chamber is brought to the pressure of the Mo zone, the valve separating the Mo zone from the lock is opened. Bringing the two zones to the same pressure is important to prevent a pressure surge in the Mo zone. The valve between Mo and the lock is closed, the lock is pumped to the pressure of the CIGS processing chamber, and then the valve between the lock and the CIGS zone is opened. Such an arrangement adds considerable unnecessary complexity to the system.

Marked-up paragraph beginning on page 44, line 17 and ending on page 45,
page 4:

Another advantage of separate chamber processing is that downtime for unscheduled maintenance for repair does not take down the entire plant. This is particularly important where there are several chambers installed for each layer because even if one CIGS is down, for example, the entire plant is not down. In addition, scheduled downtime for source replenishment does not require stopping an entire line. It is also easier to scale the processing to the desired production rate because the chambers can be independently sized, i.e., not all chambers have to run at the same rate. For example, a single Mo chamber may be able to process web fast enough for four CIGS chambers, two CdS chambers and two ITO chambers. Similarly, additional chambers can be added more easily.

Marked-up paragraph beginning on page 47, line 17 and ending on page 48,
line 4:

It should be noted that crucibles of structures 70, 72, 74, sparger tubes 76, 78, 79, 81, and the respective nozzles associated with these structures, are collectively substantially centered on the footprint of zone R (its W and Z dimensions). Preferably, the width W of zone R is somewhat greater than the width of the traveling strip material, and laterally [speaking], the width dimension of the strip material is substantially centered on width W. Consequently, the lateral boundaries, or edges, of the strip material are completely within zone R, and as strip material passes through the zone, it is treated to a generally bilaterally symmetrical engagement with the vapor components being

deposited. The bilateral symmetry just mentioned is such symmetry viewed relative to the long axis 24a of chamber 24. See Fig. 9.

Marked-up paragraph beginning on page 50, line 20 and ending on page 51, line 3:

The CIGS layer created with either chamber organization (Figs. 6 and 12) has an internal make-up or composition of approximately 23.5 atomic percent copper, 19.5 atomic percent indium, 7 atomic percent gallium, and 50 atomic percent selenium. The key difference is the CIGS formed in the chamber of Fig 12 better tolerates mechanical stresses imparted on the film as a consequence of fabricating the unique flexible photovoltaic device disclosed herein.

Marked-up paragraph beginning on page 53, line 1 and ending on page 53, line 12:

Several source orders have been investigated to achieve the optimum composition. An alternative construction for chamber 24 is illustrated in Figs. 12-14. The primary distinction, relative to the first-described chamber-24 construction, is the use of five rather than three elongate, heated, vapor-delivery effusion sources [82, 84, 86, 88 and 90]86, 88, 90, 92 and 94 (generally like previously discussed effusion sources 70, 72, 74). It should be noted that a space with no vapor source is provided between second and third effusion sources. The nozzles (three each) in the central vessel [86] 90 delivers copper vapor; those in effusion sources [82 and 88] 86 and 92 delivery gallium vapor; and those in vessels [84 and 90] 88 and 94 deliver indium vapor. An additional modification includes a final gallium [resulting] deposition employed after the final

indium in Figs. 12-14, more will be said about this alternative possibility later -- a special alternative which can be thought of as possessing “longitudinal vapor (material)-delivery symmetry”.

Marked-up paragraph beginning on page 53, line 13, and ending on page 54, line 7:

Thus, each point on the surface of a strip passing through this version of chamber 24 encounters, in sequence: a gallium/indium-rich region, a copper-rich region, and finally, another indium/gallium-rich region. This “encounter” experience can be thought of as involving a kind of longitudinal material-deposition symmetry within zone R. Similar to the three source example, instantaneous flux of a point on the strip can be plotted as a function of position in Zone R, as graphically shown in Figs. 38 and 39. As was mentioned above, the respective vapor effusion rates of the five effusion sources [82, 84, 86, 88, 90] 86, 88, 90, 92 and 94 respectively, are controlled in such a fashion that the entrance end of zone R is indium-gallium, the middle region of this zone is copper-rich, and the exit end of the zone is gallium-indium-rich, as graphically illustrated in Fig. 40. In particular, we have found that, by establishing appropriate effusion rates for all sources: (a), within the entrance end of zone R, the ratio $(\text{Cu})/(\text{Ga}+\text{In})$ is generally about 0.0, and the ratio $(\text{Ga})/(\text{Ga}+\text{In})$ is generally about 0.35; (b), within the middle region of zone Z above the copper source, the ratio $(\text{Cu})/(\text{Ga}+\text{In})$ is generally about 1.1, and the ratio $(\text{Ga})/(\text{Ga}+\text{In})$ is generally about 0.2; and (c), within the exit end of zone Z, the ratio $(\text{Cu})/(\text{Ga}+\text{In})$ is generally between 0.8 and 0.92, most preferably, about 0.88, and the ratio $(\text{Ga})/(\text{Ga}+\text{In})$ is between generally between 0.25 and 0.3, most preferably 0.275.

Marked-up paragraph beginning on page 54, line 8 and ending on page 55, line 5:

In accordance with a preferred embodiment of the system of the present invention, the molten temperature of gallium within crucible [82] 86 is suitably maintained in the range of about 1000°C to about 1350°C, and most preferably at a temperature of about 1120°C (+/- about 1°C). The temperature of the molten indium within crucible [84] 88 is suitably maintained within the range of about 950°C to about 1300°C, and most preferably at about 1130°C (+/- about 1°C). The temperature of the molten copper within crucible 86 is suitably maintained within the range of about 1350°C to about 1700°C, and most preferably at about 1496°C (+/- about 1°C). The temperature of the molten gallium within crucible [88] 92 is suitably maintained within the range of about 1000°C to about 1350°C, and most preferably at about 1130°C (+/- about 1°C). Finally, the temperature of the molten indium within crucible [90] 94 is most appropriately (according to what we have learned in our practice of use of this invention) maintained in the range of about 950°C to about 1300°C, and most preferably at about 1055°C (+/- about 1°C). The temperature of molten selenium in reservoir 85b is preferably maintained in the range of about 275°C to about 500°C, and most preferably to about 415°C (+/- about 0°C). As stated before, [although]although these temperatures are in the preferred range for the disclosed sources with 0.95-cm orifices, the rate restricting nozzle principals outlined herein indicated that as the orifice [size] increases, the temperature would decrease to achieve a constant rate, or alternatively, as the orifice size decreases, the temperature would increase to achieve a constant rate.

Marked-up paragraph beginning on page 55, line 21 and ending on page 56,
line 14:

Differentiating reasons for choosing to employ, for example, one or the other of these two illustrated arrangements are outlined below. For the three source arrangement, principal advantages include simplified control of three sources, ensuring the copper rich stage which is an important factor in achieving high efficiency, however, controlling adhesion of the CIGS deposited by the three source technique to substrates with a large coefficient of thermal expansion mismatch with the absorber is difficult. Additionally, the three source arrangement is more likely to lead to through thickness composition variations that may limit the photovoltaic device performance. Principal advantages of the five source arrangement are improved adhesion, even with substrates with a large CTE mismatch to CIGS, and greater ability to tailor the through thickness composition to enhance the photovoltaic device performance. The key challenge with the five source arrangement is controlling the relative fluxes of indium and gallium on either side of the centrally located copper source [90]. We further recognize that other considerations might well dictate a preference for selecting and implementing an altogether different distributed vapor-plume layout, and these other kinds of approach can certainly be determined easily by those skilled in the art in view of the present disclosure.

Marked-up paragraph beginning on page 56, line 15 and ending on page 57,
line 9:

Typically, the exposed surface of a deposited CIS or CIGS layer will have a quite irregular, three-dimensional surface topography, with such topography being

characterized by many randomly distributed peaks and valleys. The character of this surface is the primary determinant of the desirability of utilizing an i-ZnO layer immediately underneath the final, conductive ZnO:Al layer. It is important that the CdS layer completely separates the CIS layer from the top contact layer. Therefore, where the CdS layer alone provides adequate [separate] separation, no supplemental insulating layer is necessary. However, where the CdS layer does not sufficiently cover the CIS layer, the i-ZnO layer can provide such separation. As was mentioned earlier, the present invention avoids the necessity of using a CdS wet-dipping technique – favoring instead, and preferably, the application of the CdS layer by way of RF-sputtering. However, the resulting CdS layer is thinner and less certain to completely isolate the two layers it lies between. This issue is more significant where a typical, prior art, wet-dipping technique for applying a layer of CdS is not used. With RF-sputtering preference, it is generally desirable, at least in certain instances, to include such an i-ZnO intermediary layer. Determination, of course, about whether to include, or not to include, this layer is dependent on the particular application and is a matter of design choice.

Marked-up paragraph beginning on page 57, line 10 and ending on page 57, line 13:

The chamber-representing blocks 26, 28 and 30 illustrated in Fig. 11 can be viewed, as has been mentioned, as illustrating the steps, and the equipment employed therefore, involved in creating (a) the mentioned CdS layer, (b) the mentioned optional i-ZnO layer, and (c) the final conductive-oxide ZnO:Al over-layer.

Marked-up paragraph beginning on page 58, line 12 and ending on page 58, line 19:

RF-sputtering of the CdS layer employs an appropriate CdS target, and this sputtering takes place preferably at an RF frequency of 13.5-MHz. The power level employed for sputtering is chosen to coordinate layer-formation activity with a selected strip linear transport speed to achieve the desired CdS layer thickness. An appropriate transport speed lies in the range of about 1.0-cm-per-minute to about 2-meters-per-minute, and a transport speed of about 30-cm-per-minute is particularly suitable. Within this strip transport speed, appropriate RF power ranges are between 100 and 1200 watts, most appropriately at 300 watts.

Marked-up paragraph beginning on page 58, line 20 and ending on page 59, line 3:

Following CdS-layer formation, the take-up roll [(un-numbered)] 60 from chamber 26 which now contains a layer structure including CdS is transferred to another isolated processing chamber 28 of Fig. 11, wherein the optional intermediary i-ZnO layer is created. This layer is established utilizing a DC sputtering technique to achieve a final layer thickness preferably in the range of about 100- to about 1000-Angstroms, and most preferably about 400-Angstroms.